

## Quantifying noise levels of intercellular signals

Kai Wang, Wouter-Jan Rappel, Rex Kerr, and Herbert Levine

Center for Theoretical Biological Physics, University of California San Diego, La Jolla, California 92093-0319, USA

(Received 12 January 2007; revised manuscript received 18 April 2007; published 5 June 2007)

Cells often measure their local environment via the interaction of diffusible chemical signals with cell surface receptors. At the level of a single receptor, this process is inherently stochastic, but cells can contain many such receptors which can reduce the variability in the detected signal by suitable averaging. Here, we use explicit Monte Carlo simulations and analytical calculations to characterize the noise level as a function of the number of receptors. We show that the residual level approaches zero and that the correlation time, i.e., the waiting time needed to obtain statistically independent data, diverges, both for large receptor numbers. This result has important implications for such processes as eukaryotic chemotaxis.

DOI: [10.1103/PhysRevE.75.061905](https://doi.org/10.1103/PhysRevE.75.061905)

PACS number(s): 87.10.+e, 87.16.Ac, 87.16.Xa

### I. INTRODUCTION

The interaction between an external diffusing stimulus and cell receptors has long been recognized as a stochastic process [1]. At the level of a single receptor, this process is inherently stochastic, but cells can contain many such receptors which can reduce the variability in the detected signal by suitable averaging. It is therefore of interest to characterize the residual noise in this measurement as a function of interaction kinetics, signal integration time, and receptor number.

In their classic paper on the physics of chemoreception, Berg and Purcell [2] argued for an irreducible level of noise encountered whenever a cell utilizes receptors to detect local concentrations of diffusing molecules. Using heuristic arguments, they proposed that for large receptor number the normalized variance in the estimated concentration  $c$  approaches

$$\left(\frac{\delta c}{\bar{c}}\right)^2 \approx \frac{1}{DT\bar{c}R}. \quad (1)$$

Here  $D$  is the diffusivity of the molecule with mean concentration  $\bar{c}$ ,  $R$  is the cell radius, and  $T$  is the measurement time, implemented by the downstream signaling circuitry. This result was re-derived by Bialek and Setayeshgar by using a fluctuation-dissipation approach [3]. This leaves the impression that a cell cannot achieve arbitrary accuracy by increasing its receptor number; its only option would be to increase the measurement time  $T$ , which may be an impractical solution for a dynamically changing environment. Here we will show by direct stochastic simulation and by physical reasoning that the above result is valid if the measurement time is much larger than the receptor array correlation time  $\tau_c$  but needs to be revisited when  $T$  is smaller than  $\tau_c$ . Furthermore, we will show that this correlation time scales with receptor number  $N$  and hence Eq. (1) will break down if  $T$  is held fixed and the number of receptors is increased.

### II. MODEL

We start by focusing on the most common interaction between a ligand  $L$  and a receptor:



The forward rate  $k_+[L]$ , where  $[L]$  represents the ligand concentration, and backward rate  $k_-$  determine the transitions between the unoccupied  $R_0$  and occupied  $R_1$  states and can be combined to give the dissociation constant  $K_d \equiv \frac{k_-}{k_+}$ .

To study the stochastic dynamics of this model, we performed numerical simulations using MCell3, a modeling tool for realistic simulation of cellular signaling in complex three dimensional geometries [4]. MCell uses highly optimized Monte Carlo algorithms to track the stochastic behavior of discrete molecules in space and time as they diffuse in user-specified geometries. It can model interactions between diffusing molecules and receptors on cell membranes as well as molecule-molecule interactions and has been validated extensively [4].

In our simulations, we modeled the cell as a  $5\text{-}\mu\text{m}$  radius sphere, rendered by 100 triangles. The surface of the cell was divided into tiny patches and each patch could hold at most one receptor. The patch density was taken to be  $1000/\mu\text{m}^2$ , resulting in a receptor size of  $1000\text{ nm}^2$ . We have verified that simulations with smaller receptor sizes show no observable differences for the parameters we are considering here. A variable number of  $N$  receptors ( $N=20\,000\text{--}300\,000$ ) were randomly distributed on the membrane of the cell. Each receptor can bind one ligand and the dissociation constant was taken to be  $K_d=30\text{ nM}$  and the unbinding rate as  $k_-=10\text{ s}^{-1}$ . Our cell was placed in a cubic box with sides of size  $30\text{ }\mu\text{m}$  with a ligand concentration of  $\bar{c}=1\text{ nM}$ , independent of the number of receptors [13].

Each simulation simulated 50 s and the time step was  $10\text{ }\mu\text{s}$ . At the start of a simulation, a certain amount of ligand molecules are released into the box and diffuse freely with diffusion constant  $D=200\text{ }\mu\text{m}^2/\text{s}$ . Once a ligand hits a receptor, it can either bind to it or be reflected off the membrane. MCell3 calculates the binding probability based on the reaction rates, ligand diffusivity, receptor size, and time step. After an initial transient period of 10 s, during which the system reaches equilibrium, the number of bound receptors was recorded every 1 ms. A typical snapshot of a simulation is presented in Fig. 1. We have verified that our results

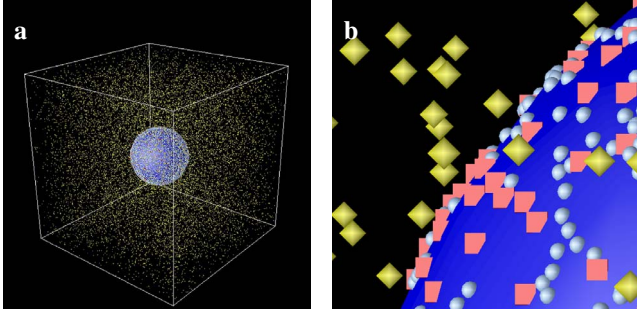


FIG. 1. (Color online) Representation of the numerical geometry. (a) A spherical cell is placed at the center of the computational box. (b) A closeup view of the membrane with its receptors and diffusing ligands. Bound receptors on the cell membrane are plotted red cubes, unbound are plotted as white spheres and freely diffusing ligands are yellow diamonds.

do not change significantly by changing either the time step size or the box size.

For each simulation, we measured the instantaneous number of bound receptors  $Z(t) = \frac{1}{N} \sum_i^N r_i$  (where  $r_i$  is a binary random variable taking the value 0 if the  $i$ th receptor is in the  $R_0$  state and 1 if the  $i$ th receptor is in the  $R_1$  state) along with its average and variance. In addition, we calculated the correlation function  $C(\tau) = \int [Z(t) - \bar{Z}][Z(t+\tau) - \bar{Z}] dt$ . The latter is only calculated for  $\tau < 4$  s; for larger values of  $\tau$  the correlation function is overwhelmed by fluctuations. The ensemble average and variance of these quantities are estimated by repeating each simulation ten times. The ensemble average of the correlation function is fit to an exponential,  $C(\tau) \sim \exp(-\tau/\tau_c)$ , to obtain an estimate of the correlation time scale  $\tau_c$ .

### III. RESULTS

Figure 2(a) shows the variance  $\sigma_Z^2$  of  $Z$  as a function of receptor number. The data are easily fit by the form  $\sigma_Z^2 = A_0/N$  with the coefficient  $A_0$  equal to

$$A_0 = \frac{\bar{c}K_d}{(\bar{c} + K_d)^2} \quad (3)$$

which is just the single receptor variance. This simple finding arises from the fact that once a molecule binds a receptor, it cannot affect neighboring receptors no matter how close-by they are located, until a finite time later when it is unbound. Hence instantaneous measurements at separate receptors are uncorrelated and the mean has accuracy that scales as  $1/N$ . Thus utilizing a one-time measurement, the cell can attain arbitrary accuracy in its evaluation of a signal concentration.

To understand why this result appears to disagree with the Berg-Purcell conclusion, we consider now the time-averaged measurements,

$$Z_T(t) = \frac{1}{T} \int_{t-T}^t d\tau Z(\tau), \quad (4)$$

where  $T$  is the time interval over which the instantaneous measurement is averaged. As demonstrated in Fig. 2(b), the

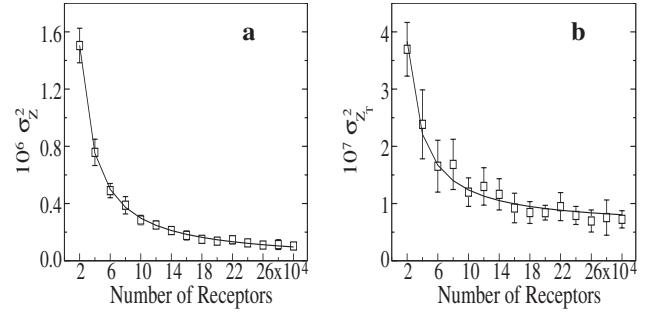


FIG. 2. Instantaneous measurements of receptor occupancy can achieve arbitrary accuracy while time-averaged measurements display a residual noise level. (a) The variance of instantaneous measurements of receptor occupancy as a function of the number of receptors  $N$ . The symbols show the results from our MCell3 simulations which agree very well with the expression  $\sigma_Z^2 = \bar{c}K_d / (N(\bar{c} + K_d)^2)$ , shown as a solid line. The error bars here, and in (b), indicate the standard deviation obtained by performing ten independent simulations. (b) The variance of time-averaged measurements as a function of the number of receptors. Shown are the results of the simulations (symbols) and the fitting formula  $A_T/N + B_T$  with  $A_T = 6.49 \times 10^{-3}$ , in good agreement with Eq. (10), and  $B_T = 5.83 \times 10^{-8}$ . The instantaneous receptor occupancy was averaged over  $T = 1$  s.

data now do fit the expected finite residual formula  $\sigma_{Z_T}^2 = A_T/N + B_T$ ; the error cannot be less than  $B_T$ . The difference between the instantaneous measurement and the time averaged measurement is more easily appreciated when we write the variance as  $\sigma^2 = A(1/N + 1/N_c)$ . For the time averaged measurement we obtain  $N_c = 1.1 \times 10^5$  while the instantaneous measurement results in a value of  $N_c$  that is nearly two orders of magnitude bigger ( $N_c = 7.6 \times 10^6$ ).

How can this occur? The answer is that as long as the integration time  $T$  is longer than the correlation time  $\tau_c$  one needs to multiply the instantaneous data by a factor of  $2\tau_c/T$  to obtain the time-averaged measurement. To see this, we start with the definition of the variance of the time-averaged measurement:

$$\begin{aligned} \sigma_{Z_T}^2 &= \left\langle \left( \frac{1}{T} \int_0^T [Z(t) - \bar{Z}] dt \right)^2 \right\rangle \\ &= \frac{1}{T^2} \int_0^T dt \int_0^T ds \langle Z(t)Z(s) \rangle - \bar{Z}^2. \end{aligned} \quad (5)$$

Next, we assume that the correlation function has an exponential decay:

$$\langle Z(t)Z(s) \rangle = \bar{Z}^2 + \sigma_Z^2 e^{-|t-s|/\tau_c},$$

where  $\tau_c$  is the correlation time. Performing the integrals leads to

$$\sigma_{Z_T}^2 = \frac{2\sigma_Z^2\tau_c}{T^2} [T - \tau_c(1 - e^{-T/\tau_c})]. \quad (6)$$

The relationship between the two variances can be simplified for  $T \gg \tau_c$  where it becomes  $\sigma_{Z_T}^2 = \frac{2\sigma_Z^2\tau_c}{T}$ . Thus to obtain the

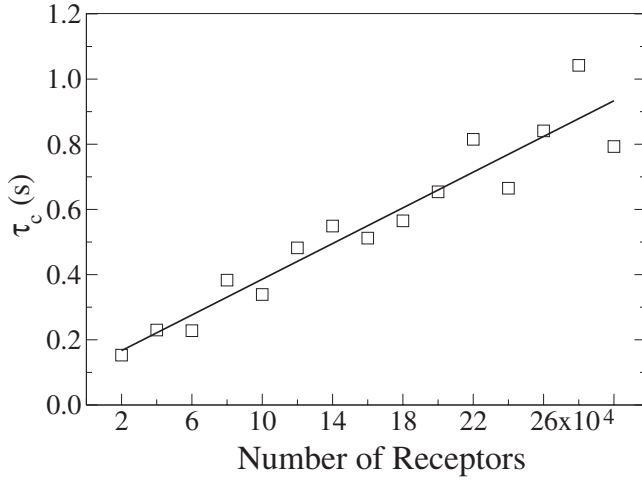


FIG. 3. The correlation time of receptor occupancy increases linearly with the number of receptors. Symbols represent the correlation time obtained from fitting the measured correlation function to an exponential decay function. The solid line shows the linear fit  $\tau_c(N) = \tau_0 + \Lambda N$  with  $\tau_0 = 0.112$  s and  $\Lambda = 2.74 \times 10^{-6}$  s.

variance of the time-averaged measurement, one needs to multiply the variance of the instantaneous measurement with the correlation time. For our system, this correlation time *diverges* as  $N$  for large receptor number which can be demonstrated directly in our simulations (Fig. 3). Hence  $\tau_c \sim \Lambda N$  which leads to the residual term

$$B_T = \frac{2\Lambda A_0}{T}, \quad (7)$$

consistent with our computational data.

Where does this diverging time come from? The receptor surface density for our cell is obviously  $\rho = N/4\pi R^2$ . Thus the expected number of bound receptors per unit surface area is  $\rho\bar{c}/K_d$ , where for simplicity we have considered the case  $\bar{c} \ll K_d$ , leading to  $A_0 = \bar{c}/K_d$ . In order for the molecules bound to these receptors to escape to infinity and hence for the configuration to be completely refreshed, we must wait a time equal to the correlation time:

$$\tau_c = \frac{1}{k_-} + \frac{\rho\bar{c}/K_d}{J_{diff}} = \frac{1}{k_-} + \frac{N}{4\pi DRK_d}, \quad (8)$$

where the first term describes the average time for unbinding and where the diffusive flux is given by  $J_{diff} = D\bar{c}/R$ . We have verified these scalings through direct simulations. Combining all these, we immediately find

$$\sigma_{Z_T}^2 = \frac{A_T}{N} + B_T = \sigma_Z^2 \frac{2\tau_c}{T} = \frac{2A_0}{NT} \left( \frac{1}{k_-} + \frac{N}{4\pi DRK_d} \right) \quad (9)$$

and thus

$$A_T = \frac{2A_0}{Tk_-} \quad \text{and} \quad B_T = \frac{\bar{c}}{2\pi DTRK_d^2}. \quad (10)$$

To compare the results we report here with Eq. (1), we first need to relate the variance in concentration level  $(\delta c/\bar{c})^2$  to the variance in the number of bound receptors  $\sigma_{Z_T}^2$ . The

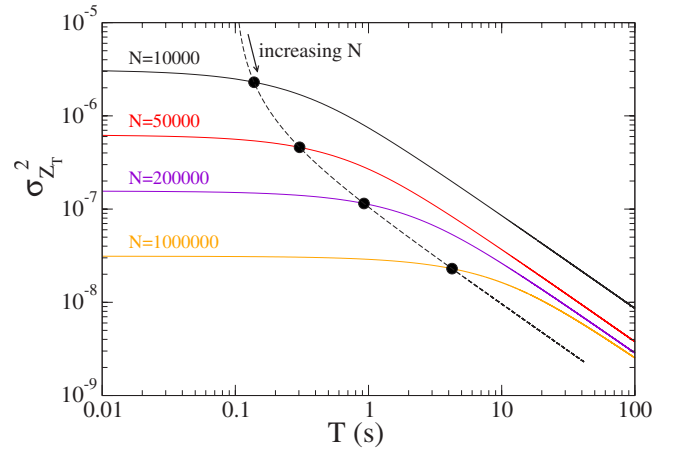


FIG. 4. (Color online) The time-averaged variance as a function of the measurement time  $T$  for different numbers of receptors. The symbols represent the points for which the measurement time equals the correlation time. The collection of these points for different  $N$  is drawn as a dashed line. Below this line, the variance approaches the instantaneous variance  $\sigma_Z^2$  while above this line the variance scales as  $1/T$ .

average occupancy level is given by  $\bar{Z} = \bar{c}/(\bar{c} + K_d)$  from which we can derive  $\delta c = (\bar{c} + K_d)^2 \delta Z / K_d$ . Hence  $(\delta c/\bar{c})^2$  is simply  $\sigma_{Z_T}^2$  multiplied by a factor that depends on the average concentration and the dissociation constant:

$$\left( \frac{\delta c}{\bar{c}} \right)^2 = \sigma_{Z_T}^2 \left( \frac{(\bar{c} + K_d)^2}{\bar{c}K_d} \right)^2. \quad (11)$$

From this expression, and from Eq. (9), we see that the term  $B_T$  is in agreement with Eq. (1) for small  $\bar{c}$ . The crucial point, however, is that this formula is valid only for long-enough times ( $T > \tau_c$ ) and *does not* imply any irreducible diffusive noise limiting measurement accuracy. In fact, for any fixed measuring time  $T$ , there is a sufficiently large  $N$  such that  $\tau_c(N) > T$ , resulting in a variance that scales as  $1/N$  just like the variance of instantaneous measurements. This is demonstrated in Fig. 4 where we have plotted  $\sigma_{Z_T}^2$  as a function of the measurement time  $T$ , using Eq. (6), for different numbers of receptors. On each curve we have marked the point where  $T = \tau_c$ ; the collection of these points for different  $N$  is plotted as a dashed line. Below this line,  $T$  is much smaller than  $\tau_c$  and the time-averaged variance approaches the instantaneous variance  $\sigma_Z^2$ .

Furthermore, the difference in the noise level estimated from Eq. (1) and from our formula can become significant. In Fig. 5 we have plotted  $(\delta c/\bar{c})^2$  as a function of the diffusion constant as predicted by Eq. (1) (dashed line) and by our general formulas Eqs. (6) and (11) (solid line). For small diffusion constants, where the correlation time becomes larger than the averaging time, the difference between the two formulas becomes appreciable and a simple application of the Berg and Purcell formula would significantly overestimate the noise level.

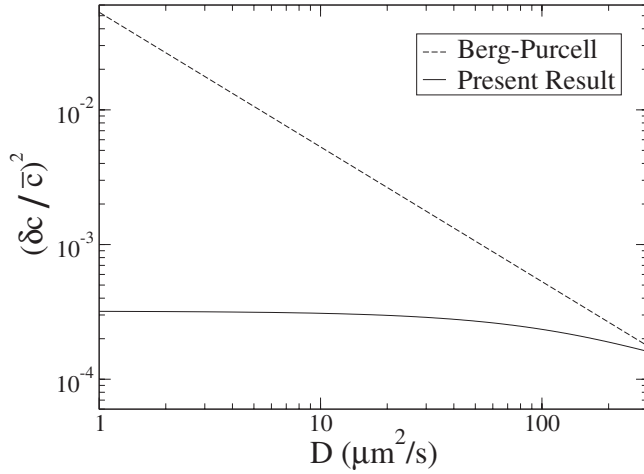


FIG. 5. The normalized variance in the concentration as a function of the diffusion constant using the Berg and Purcell result (dashed line) and found in this paper (solid line). For small diffusion constants the widely used formula of Berg and Purcell can significantly overestimate the noise level. Parameter values are the default ones with  $N=100\,000$  and  $T=1$  s.

#### IV. ALTERNATIVE REACTION MODELS

It is interesting to note that our conclusions depend on the interaction details. To study this, we considered an alternate model in which the diffusing molecule  $L$  acts enzymatically on the receptor:



where the forward and backward rates are identical to the ones in the binding-unbinding model. Now, the fact that the diffusing particle is not absorbed by the receptor means that it can act in rapid succession on neighboring receptors, thereby correlating their response. In the limit of infinite  $N$ , this can happen with infinitesimal time lags and the resulting correlations limit the achievable accuracy as is shown in Fig. 6 (red curve). In other words, in this model the variance of the instantaneous measurement does not vanish for large  $N$  but remains finite.

It is not clear whether there are any direct realizations of this alternate scheme. However, more complex models in which the decay of the bound ligand-receptor pair leaves the receptor at least temporarily in the signaling-competent state will behave in the enzymatic way whenever the dissociation rate is fast compared to the final rate of decay. To further investigate the different limits represented by these two interaction schemes, we invented an interpolating model. In this model, a ligand binds to a receptor with rate  $k_+[L]$  and unbinds with a rate  $k_1$ . Following the unbinding of the ligand, however, the receptor remains “active” and decays to its inactive form with rate  $k_2$ . Thus this scheme can be written as

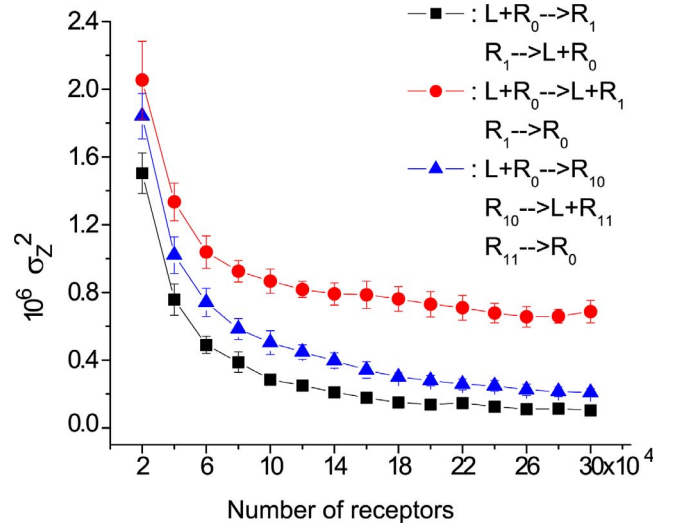


FIG. 6. (Color online) The variance of the instantaneous receptor occupancy for three types of receptor-ligand interactions. Black symbols: binding-unbinding scheme with the default rates ( $K_d=30$  nM,  $k_+=0.33$  nM $^{-1}$  s $^{-1}$ ,  $k_-=10$  s $^{-1}$ ). Red symbols: enzymatic scheme for the same rates. Blue symbols: interpolating scheme with  $k_+=0.33$  nM $^{-1}$  s $^{-1}$ ,  $k_1=20$  s $^{-1}$ ,  $k_2=20$  s $^{-1}$ .



To ensure an identical equilibrium concentration we have to choose

$$\frac{1}{k_1} + \frac{1}{k_2} = \frac{1}{k_-} \quad (17)$$

and the measurement for the bound receptor state now comprises the sum of the two active forms  $R_{10}$  and  $R_{11}$ . It is easy to see that if  $k_2$  goes to infinity, we recover the binding-unbinding model while if  $k_1$  goes to infinity, we recover the enzymatic model. Thus this scheme affords a smooth interpolation between the two extreme cases. Indeed, Fig. 6 shows that the variance for this model, plotted as blue triangles, falls between the two limiting cases.

#### V. DISCUSSION

The new understanding of the way in which fluctuations limit measurement accuracy will become relevant whenever cells utilize measurements with integration times less than the receptor array correlation  $\tau_c$ . Of course, such measurements will be strongly correlated. However, the integration time  $T$  is determined by the downstream signaling pathways and, unlike  $\tau_c$ , cannot be varied by changing external parameters. Hence cells will sometimes operate in the regime discussed in this paper. The most intriguing possible example arises in the case of the chemotactic sensing of f-Met-Leu-Phe by neutrophils [5]. Eukaryotic chemotaxis is a difficult task, as the signal is created by a small difference between front and rear concentrations whereas the noise is due to the mean occupancy [6]. Typical interaction numbers for this

system are  $k_{-} \approx 2/s$ ,  $K_d \approx 15\text{--}50$  nM, for a cell of radius  $6\text{--}8$   $\mu\text{m}$  [7,8]. The number of receptors is regulated, increasing from  $N=40\,000$  to  $N=150\,000$  when the neutrophil is activated by cytokines [9,10]. With a typical small-molecule diffusivity of  $200$   $\mu\text{m}^2/s$ , we estimate a  $\tau_c$  of approximately  $1$  s, but this could be increased by experimental manipulation of the extracellular medium. Rapidly advancing microfluidics technology [11,12] should enable a test of whether and when the neutrophil sensing must be thought of as in-

stantaneous, being governed directly by the individual receptor variance.

#### ACKNOWLEDGMENTS

We thank T. M. Bartol, Jr. and T. J. Sejnowski for useful discussions. This work was supported by the National Science Foundation Physics Frontier Center-sponsored Center for Theoretical Biological Physics.

- 
- [1] D. Bray, *Nature (London)* **376**, 307 (1995).  
 [2] H. C. Berg and E. M. Purcell, *Biophys. J.* **20**, 193 (1977).  
 [3] W. Bialek and S. Setayeshgar, *Proc. Natl. Acad. Sci. U.S.A.* **102**, 10040 (2005).  
 [4] J. R. Stiles and T. M. Bartol, in *Computational Neurobiology: Realistic Modeling for Experimentalists*, edited by E. de Schutter (CRC Press, Boca Raton, FL, 2001), pp. 87–127.  
 [5] H. R. Bourne and O. Weiner, *Nature (London)* **419**, 21 (2002).  
 [6] L. Song, S. M. Nadkarni, H. U. Bödeker, C. Beta, A. Bae, C. Franck, W.-J. Rappel, W. F. Loomis, and E. Bodenschatz, *Eur. J. Cell Biol.* **85**, 981 (2006).  
 [7] J. A. Adams, G. M. Omann, and J. J. Linderman, *J. Theor. Biol.* **193**, 543 (1998).  
 [8] P. S. Chang, D. Axelrod, G. M. Omann, and J. J. Linderman, *Cell Signal* **17**, 605 (2005).  
 [9] R. H. Weisbart, D. W. Golde, and J. C. Gasson, *J. Immunol.* **137**, 3584 (1986).  
 [10] S. D. Tennenberg, F. P. Zemlan, and J. S. Solomkin, *J. Immunol.* **141**, 3937 (1988).  
 [11] D. J. Beebe, G. A. Mensing, and G. M. Walker, *Annu. Rev. Biomed. Eng.* **4**, 261 (2002).  
 [12] N. L. Jeon, H. Baskaran, S. K. Dertinger, G. M. Whitesides, L. V. de Water, and M. Toner, *Nat. Biotechnol.* **20**, 826 (2002).  
 [13] To reduce finite-box effects and to save computation time, we incorporated a specific concentration-clamp boundary condition in MCell3. In this condition, we imagine our computational box to be immersed in a much larger box with the same ligand concentration that functions as a reservoir. Molecules from this reservoir can enter the computational box at a random location and at a rate that equals the escape rate of molecules from the computational box to the reservoir. The latter can be calculated analytically and depends on system parameters and the time step.